# Structural and electronic properties of the wide-gap $Zn_{1-x}Mg_xS$, $Zn_{1-x}Mg_xSe$ and $Zn_{1-x}Mg_xTe$ ternary alloys



2005 J. Phys.: Condens. Matter 17 7077

(http://iopscience.iop.org/0953-8984/17/44/001)

INSTITUTE OF PHYSICS PUBLISHING JOURNAL OF PHYSICS: CONDENSED MATTER

J. Phys.: Condens. Matter **17** (2005) 7077–7088 doi:10.1088/0953-8984/17/44/001

# Structural and electronic properties of the wide-gap $Zn_{1-x}Mg_xS$, $Zn_{1-x}Mg_xSe$ and $Zn_{1-x}Mg_xTe$ ternary alloys

**Z Charifi[1,4], F El Haj Hassan[2], H Baaziz[1], Sh Khosravizadeh[3], S J Hashemifar[3] and H Akbarzadeh[3]**

[1] Physics Department, Faculty of Science and Engineering, University of M'sila, 28000 M'sila, Algeria
[2] Laboratoire de Physique de Matériaux, Faculté des Sciences (I), Université Libanaise, Elhadath, Beirut, Lebanon
[3] Department of Physics, Isfahan University of Technology, Isfahan 84154, Iran

E-mail: charifi_z@yahoo.fr

Received 27 August 2005, in final form 25 September 2005
Published 17 October 2005
Online at stacks.iop.org/JPhysCM/17/7077

**Abstract**

$Zn_{1-x}Mg_xS$, $Zn_{1-x}Mg_xSe$ and $Zn_{1-x}Mg_xTe$ ternary wide-gap semiconductor alloys were investigated using the full potential–linearized augmented plane wave (FP-LAPW) method. We have studied the effect of composition on structural properties such as lattice constants, bulk modulus and bond ionicity. The bandgap and the microscopic origins of compositional disorder have also been explained in detail. In addition, from the obtained band structures, the electron (hole) conduction and valence effective masses are deduced. These parameters were found to depend non-linearly on alloy composition $x$, except the lattice parameter for $Zn_{1-x}Mg_xS$, which follows Vegard's law. The calculated band structures for all three alloys show a direct bandgap in the whole range of $x$ composition. We have paid special attention to the disorder parameter (gap bowing). Using the approach of Zunger and co-workers, we have concluded that the total bandgap energy bowing was mainly caused by the charge exchange effect for the alloys of interest.

## 1. Introduction

II–VI semiconductors have been of growing interest because of their wide bandgap character and the potential applications for optoelectronic devices. Their bandgap energy falls between 1 and 3 eV, making them useful for application in optoelectronic devices in the visible region of the spectrum [1]. These materials have also been exploited both for quantum confinement

[4] Author to whom any correspondence should be addressed.

  

and for achieving waveguides. Promising candidates are $Zn_{1-x}Mg_xSe$ [2], $Zn_{1-x}Mg_xS$ [3] and $Zn_{1-x}Mg_xTe$ [4], since their energy gaps and lattice constants can be varied in a wide range by adjusting the content of stoichiometry parameter $x$. Blue–violet electroluminescence obtained from $Zn_{1-x}Mg_xSe$ bulk crystals has shown that this material could be also used for short-wavelength light-emitting devices [4]. A blue–green laser based on Mg-containing II–VI semiconductors operated continuously at room temperature with a lifetime exceeding 100 h has already been demonstrated [5, 6]. Several Schottky barrier photodetectors using $Zn_{1-x}Mg_xS$ as the active layer were fabricated; they could be used as the active material for detection of UV radiation shorter than 300 nm [7, 8]. The optical properties of $Zn_{1-x}Mg_xSe$ and $Zn_{1-x}Mg_xTe$ alloys have also been investigated experimentally [9].

The theoretical studies have been made for $Zn_{1-x}Mg_xSe$ by many researchers, using the empirical [10–13] and *ab initio* [14–16] pseudopotential methods. To the best of our knowledge there are no theoretical reports in the literature on the structural and electronic properties of $Zn_{1-x}Mg_xS$ and $Zn_{1-x}Mg_xTe$ alloys.

To obtain commercial optoelectronic devices with a long lifetime by using $Zn_{1-x}Mg_xS$, $Zn_{1-x}Mg_xSe$ and $Zn_{1-x}Mg_xTe$ ternary alloys or by related quaternary layers, we need to have a deeper understanding of the structural and electronic properties of these materials. Hence the knowledge of bulk-crystal structural properties yields useful information for engineering of the optoelectronic semiconductor devices. Therefore, the main aim of the present study was to investigate the electronic and structural properties of $Zn_{1-x}Mg_xS$, $Zn_{1-x}Mg_xSe$ and $Zn_{1-x}Mg_xTe$ ternary alloys in cubic phase over a wide range of compositions $0 \leqslant x \leqslant 1$ by using the full potential–linearized augmented plane wave (FP-LAPW) method. Various quantities, including lattice parameters, bulk modulus, bandgap, optical bowing, bond ionicity character and effective masses, were obtained for these alloys.

The organization of this paper is as follows: we describe the FP-LAPW computational details in section 2. In section 3, results and discussion for structural and electronic properties are presented. Finally conclusion is given in section 4.

## 2. Method of calculations

Describing random alloys by periodic structures will clearly introduce spurious correlations beyond a certain distance ('periodicity errors'). Preventing this problem needs a very large supercell (e.g. $>10^3$ atoms for a binary alloy), for which first-principle self-consistent calculations are still impractical. However, many physical properties of solids are characterized by microscopic length scales and local randomness of alloys and modifying the large scale randomness of alloys does not affect them. Recently, Zunger *et al* [17] implemented this fact to construct the 'special quasirandom structures' (SQS) approach by the principle of close reproduction of the perfectly random network for the first few shells around a given site, deferring periodicity errors to more distant neighbours. They argued that this approach, which we have adopted in our calculation, effectively reduces the size of the supercell for studying many properties of random alloys.

The calculations were performed by the full potential–linearized augmented plane wave (FP-LAPW) method to solve the Kohn–Sham equations as implemented in the WIEN2K code [18]. The exchange–correlation contribution was described within the generalized gradient approximation (GGA) proposed by Perdew *et al* [19] to calculate the total energy, while for electronic properties in addition to that the Engel–Vosko (EVGGA) formalism [20] was also applied. In the FP-LAPW method the wavefunction, charge density and potential are expanded differently in two regions of the unit cell. Inside the non-overlapping spheres of radius $R_{MT}$ around each atom spherical harmonic expansion is used, and in the remaining

space of the unit cell the plane wave basis set is chosen. $R_{MT}$ values for Zn, Mg, S, Se and Te were chosen to be 2.2, 2, 2, 2.25 and 2.4 au, respectively. The maximal $l$ value for the wavefunction expansion inside the atomic spheres was confined to $l_{max} = 10$. The plane wave cut-off of $K_{max} = 8.0/R_{MT}$ was chosen for the expansion of the wavefunctions in the interstitial region for all the alloys and the binary compounds MgS, MgSe and MgTe, while for the binary compounds ZnS, ZnSe and ZnTe we have used a $K_{max} = 9.0/R_{MT}$. The charge density was Fourier expanded up to $G_{max} = 14$ (Ryd)$^{1/2}$. A mesh of 35 special $k$-points for binary compounds and 27 special $k$-points for the alloy were taken in the irreducible wedge of the Brillouin zone. Both the plane wave cut-off and the number of $k$-points were varied to ensure total energy convergence.

## 3. Results and discussion

### *3.1. Structural properties*

We first calculated the structural properties of the binary compounds ZnS, ZnSe, ZnTe, MgS, MgSe and MgTe in the zinc-blende structure. Then the alloys were modelled at some selected compositions $x = 0.25$, 0.5 and 0.75 following the SQS approach. For the composition $x = 0.25$ and 0.75 the simplest structure is an eight-atom simple cubic lattice (luzonite): the cations with the lower concentration form a regular simple cubic lattice. For $x = 0.5$, the smallest ordered structure is a four-atom tetragonal cell, corresponding to the (001) superlattice. We have also checked the chalcopyrite structure, which has a 16-atom tetragonal cell for $x = 0.5$, and the results were found to be similar to those of the (001) superlattice.

The total energy of the primitive unit cell was calculated as a function of its volume, and then by fitting the results with the Murnaghan equation of state [21] the equilibrium structural properties such as the lattice constant and the bulk modulus were obtained both for the binary compounds and their alloys. Our results for the materials of interest are compared with the available experimental and theoretical predictions in table 1.

Usually, in the treatment of alloys, it is assumed that the atoms are located at the ideal lattice sites and the lattice constant varies linearly with composition $x$ according to the so-called Vegard's law [22].

$$a(A_xB_{1-x}C) = xa_{AC} + (1-x)a_{BC} \tag{1}$$

where $a_{AC}$ and $a_{BC}$ are the equilibrium lattice constants of the binary compounds AC and BC respectively. $a(A_xB_{1-x}C)$ is the alloy lattice constant.

However, violation of Vegard's law has been reported in semiconductor alloys both experimentally [29, 30] and theoretically [31–33].

Hence, the lattice constant of alloy can be written as

$$a(A_xB_{1-x}C) = xa_{AC} + (1-x)a_{BC} - x(1-x)b. \tag{2}$$

The quadratic term $b$ stands for the bowing parameter.

As a prototype the results obtained for the composition dependence of the calculated equilibrium lattice parameter for $Zn_{1-x}Mg_xSe$ alloy are shown in figure 1. A small deviation from Vegard's law is clearly visible for this alloy with upward bowing parameter equal to $-0.03$ Å which is very close to the experimental one ($-0.07$ Å) [29]. The lattice parameter bowing for $Zn_{1-x}Mg_xTe$ alloy has also been found to be very small ($-0.02$ Å), while in the case of $Zn_{1-x}Mg_xS$ alloy our calculations exhibit an excellent agreement to Vegard's law with a lattice bowing close to zero.

The overall behaviours of the variation of bulk modulus as a function of the composition $x$ for all three alloys are very similar, hence only the curve of $Zn_{1-x}Mg_xS$ alloy is presented

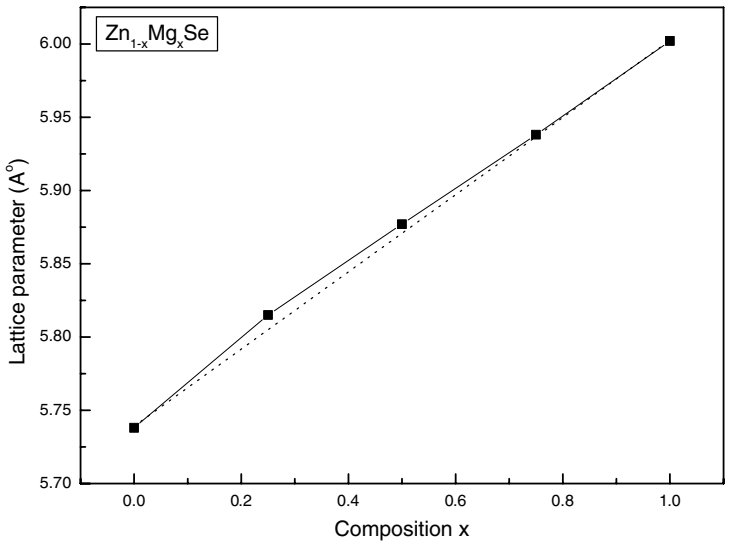


**Figure 1.** Composition dependence of the calculated lattice constant (solid squares) of $Zn_{1-x}Mg_xSe$ alloy compared with Vegard's law (dashed line).

**Table 1.** Calculated lattice parameter ($a$) and bulk modulus ($B$) for $Zn_{1-x}Mg_xS$, $Zn_{1-x}Mg_xSe$ and $Zn_{1-x}Mg_xTe$ alloys, and their binary compounds. Available experimental and theoretical data from the literature are also shown for comparison.

| | | Lattice constants $a$ (Å) | | | Bulk modulus $B$ (GPa) | | |
|---|---|---|---|---|---|---|---|
| | $x$ | Our work | Exp. | Other calculations | Our work | Exp. | Other calculations |
| $Zn_{1-x}Mg_xS$ | 1 | 5.703 | 5.62 [2] | 5.584 [25] [a]<br>5.635 [3][b] | 55.46 | | 57.5 [25][a] |
| | 0.75 | 5.644 | | | 57.66 | | |
| | 0.50 | 5.583 | | | 61.12 | | |
| | 0.25 | 5.520 | | | 65.14 | | |
| | 0 | 5.465 | 5.409 [26] | 5.427 [3][b] | 69.62 | 76.9 [24] | 77.4 [25][a] |
| $Zn_{1-x}Mg_xSe$ | 1 | 6.002 | 5.91 [29]<br>5.89 [23] | 5.873 [25][a]<br>5.86 [3][b] | 44.48 | | 47.0 [25][a] |
| | 0.75 | 5.938 | | | 47.99 | | |
| | 0.50 | 5.877 | | | 49.18 | | |
| | 0.25 | 5.815 | | | 52.96 | | |
| | 0 | 5.738 | 5.668 [43] | 5.635 [3][b] | 58.20 | 62.5 [24] | 63.9 [25][a] |
| $Zn_{1-x}Mg_xTe$ | 1 | 6.517 | 6.35 [44]<br>6.42 [4] | 6.282 [3][b] | 33.70 | | |
| | 0.75 | 6.442 | | | 35.09 | | |
| | 0.50 | 6.363 | | | 37.4 | | |
| | 0.25 | 6.284 | | | 40.79 | | |
| | 0 | 6.198 | 6.089 [43] | 6.074 [3][b] | 44.35 | 50.5 [27] | 47.7 [28][c] |

[a] *Ab initio* pseudopotential within LDA.
[b] Modified dielectric theory.
[c] Local basis set of Gaussian-type functions.

in figure 2. A significant deviation from the linear concentration dependence (LCD) with downward bowing equal to 5.83, 6.93 and 6.19 GPa for $Zn_{1-x}Mg_xS$, $Zn_{1-x}Mg_xSe$ and

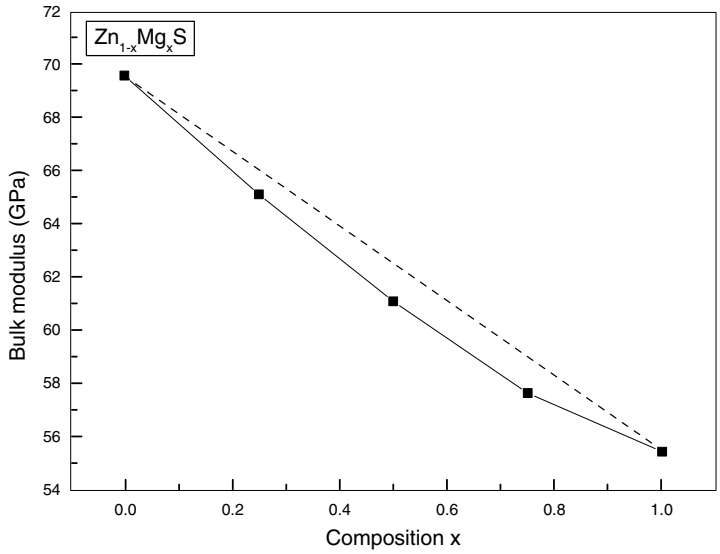


**Figure 2.** Composition dependence of the calculated bulk modulus (solid squares) of $Zn_{1-x}Mg_xS$ alloy compared with LCD prediction (dashed line).

$Zn_{1-x}Mg_xTe$ alloys, respectively, was observed. This deviation is mainly due to the mismatch of the bulk moduli of binary compounds. It is clearly seen that the bulk modulus decreases by increasing the chalcogenide atomic number. Hence, we conclude that ZnTe and MgTe are more compressible compared to the other zinc and magnesium chalcogenide compounds, respectively.

It is well known that the ionicity factor is correlated to the total valence charge density; therefore our calculations of the ionicity parameter have been carried out on the basis of the empirical model described in [34]. In figure 3, we display the ionicity of the bonds at different concentrations. It is relevant to note that for all three alloys the ionicity increases, while the bulk modulus decreases on going from $x = 0$ to 1, which is due to the increasing of magnesium concentration.

### *3.2. Electronic properties*

The calculated band structure energies of binary compounds as well as for their alloys using both GGA and EVGGA indicate a direct bandgap located at the $\Gamma$ point in the whole range of concentrations. The results are presented in table 2. It is clearly seen that the bandgap values given by EVGGA are in good agreement with the experiments. In fact, it is well known that GGA usually underestimates the energy gap [35, 36]. This is mainly due to the fact that the functionals within this approximation have simple forms that are not sufficiently flexible to accurately reproduce both exchange correlation energy and its charge derivative. Engel and Vosko by considering this shortcoming constructed a new functional form of GGA, which is able to better reproduce exchange potential at the expense of less agreement in exchange energy. This approach, which is called EVGGA, yields a better band splitting and some other properties which mainly depend on the accuracy of exchange correlation potential. On the other hand, in this method, the quantities which depend on an accurate description of exchange energy $E_x$ such as equilibrium volumes and bulk modulus are in poor agreement with experiment. The

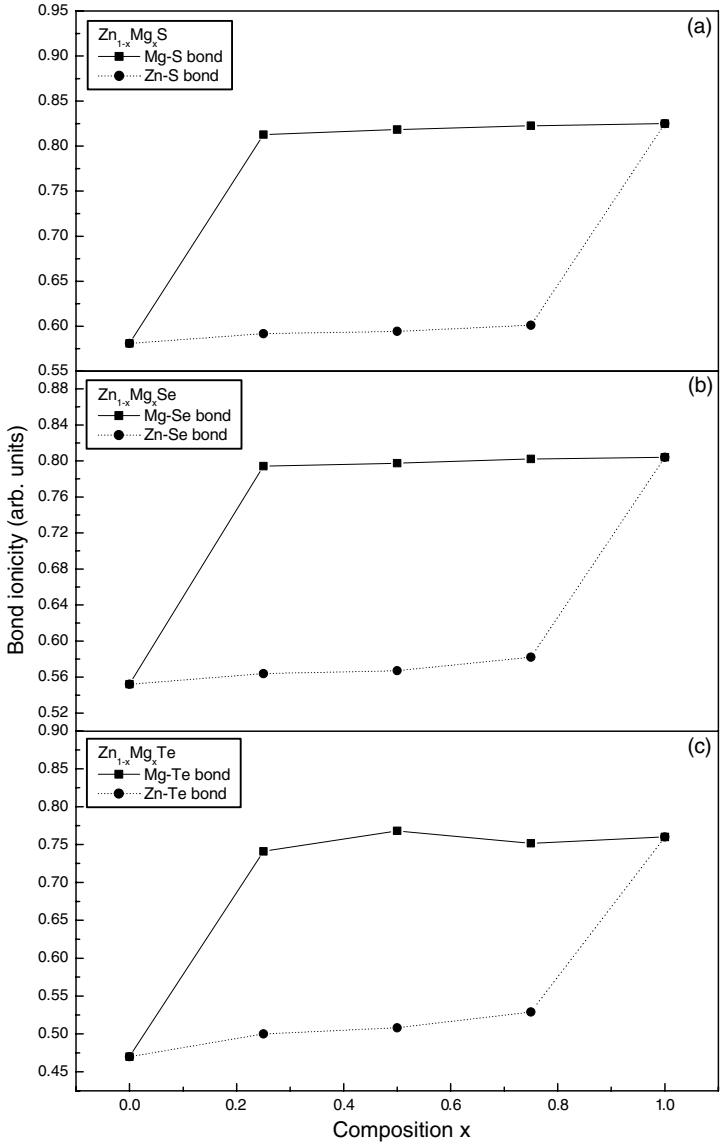


**Figure 3.** The ionicity of the bonds at different concentrations for (a) $Zn_{1-x}Mg_xS$, (b) $Zn_{1-x}Mg_xSe$ and (c) $Zn_{1-x}Mg_xTe$ alloys.

calculated bandgap $E_\Gamma^\Gamma$ for $Zn_{1-x}Mg_xS$, $Zn_{1-x}Mg_xSe$ and $Zn_{1-x}Mg_xTe$ were found to vary in the range of 2.79–4.38, 1.89–3.58 and 1.57–3.15 eV respectively.

While the lattice constant of a semiconducting alloy may follow the Vegard's rule closely, the bandgap is often found to deviate considerably from the linear average

$$E_g = xE_{AC} + (1-x)E_{BC}. \tag{3}$$

Hence it is usually expressed by

$$E_g = xE_{AC} + (1-x)E_{BC} - x(1-x)b_E \tag{4}$$

where $b_E$ is the gap bowing

**Table 2.** Bandgap energies of $Zn_{1-x}Mg_xS$, $Zn_{1-x}Mg_xSe$ and $Zn_{1-x}Mg_xTe$ alloys at different Mg concentrations (all values are in eV).

| | | $E_g$ (eV) | | | |
|---|---|---|---|---|---|
| | | Our work | | | |
| | $x$ | GGA | EVGGA | Experiment | Other work |
| $Zn_{1-x}Mg_xS$ | 1 | 3.327 | 4.385 | 4.45 [3] | 4.48 [13] 3.42 [25] |
| | 0.75 | 2.817 | 3.715 | | |
| | 0.50 | 2.509 | 3.377 | | |
| | 0.25 | 2.263 | 3.114 | | |
| | 0 | 1.953 | 2.792 | 3.68 [3] | 2.37 [25] |
| $Zn_{1-x}Mg_xSe$ | 1 | 2.517 | 3.584 | 3.6 [37] 4.0 [29] | 3.67 [13] 4.21 [11] |
| | 0.75 | 2.027 | 2.857 | | |
| | 0.50 | 1.710 | 2.512 | | 3.32 [11] |
| | 0.25 | 1.427 | 2.060 | | |
| | 0 | 1.129 | 1.889 | 2.68 [26] | 2.5 [15] 2.7 [11] |
| $Zn_{1-x}Mg_xTe$ | 1 | 2.293 | 3.156 | 3.13 [1] 3.67 [9] | 3.01 [3] |
| | 0.75 | 1.687 | 2.270 | | |
| | 0.50 | 1.456 | 2.039 | | |
| | 0.25 | 1.253 | 1.827 | | |
| | 0 | 1.012 | 1.575 | 2.28 [1] 2.39 [9] | 2.10 [3] |

Figure 4 shows the composition dependence of the calculated bandgaps using GGA and EVGGA schemes. We remark that the bandgap $E_\Gamma^\Gamma$ increases non-linearly with increasing of the Mg content providing a positive gap bowing. A similar behaviour of $E_\Gamma^\Gamma$ for $Zn_{1-x}Mg_xSe$ alloy has been observed experimentally by Jobs *et al* [29] and also theoretically using the empirical pseudopotential method [11]. Our results for the gap bowing, obtained by quadratic fits, are presented and compared with the other available experimental and theoretical predictions in table 3. The results shown in figure 4 obey the following variations:

$$Zn_{1-x}Mg_xS \Rightarrow \begin{cases} E_g^{GGA}(x) = 1.98 + 0.79x + 0.53x^2, \\ E_g^{EVGGA}(x) = 2.83 + 0.63x + 0.88x^2 \end{cases} \tag{5}$$

$$Zn_{1-x}Mg_xSe \Rightarrow \begin{cases} E_g^{GGA}(x) = 1.15 + 0.87x + 0.47x^2, \\ E_g^{EVGGA}(x) = 1.92 + 0.63x + 0.98x^2 \end{cases} \tag{6}$$

$$Zn_{1-x}Mg_xTe \Rightarrow \begin{cases} E_g^{GGA}(x) = 1.05 + 0.33x + 0.86x^2, \\ E_g^{EVGGA}(x) = 1.64 - 0.03x + 1.46x^2. \end{cases} \tag{7}$$

It has been seen that the main influence of the bandgap energy is due to the lattice constant and the electronegativity mismatch of the parent atoms [12, 29, 42].

In order to obtain the origins of bowing parameter, we adopted the approach of Zunger and co-workers [17], which decomposes it into three contributions:

$$b = b_{VD} + b_{CE} + b_{SR} \tag{8}$$

$b_{VD}$ is the volume deformation contribution, which is due to the change of lattice constants of the binary compounds to the alloy value. The chemical electronegativity contribution ($b_{CE}$) arises from the charge exchange in the alloy. $b_{SR}$ is the structural contribution due to the relaxation of the anion–cation bond lengths in the alloy.

**Table 3.** Decomposition of optical bowing into volume deformation (VD), charge exchange (CE) and structural relaxation (SR) contributions compared with that obtained by a quadratic interpolation and other predictions.

| | | Present work | | Present work Quadratic equation | | | |
|---|---|---|---|---|---|---|---|
| | | GGA | EVGGA | GGA | EVGGA | Experiment | Other work |
| $Zn_{1-x}Mg_xS$ | $b_{VD}$ | −0.099 | −0.657 | | | | |
| | $b_{CE}$ | 0.502 | 1.509 | | | | |
| | $b_{SR}$ | 0.123 | −0.007 | | | | |
| | $b$ | 0.526 | 0.845 | 0.528 | 0.880 | | |
| $Zn_{1-x}Mg_xSe$ | $b_{VD}$ | −0.065 | −0.106 | | | | 2.070 [14] |
| | $b_{CE}$ | 0.466 | 1.724 | | | | −1.459 [14] |
| | $b_{SR}$ | 0.048 | −0.689 | | | | −1.177 [14] |
| | $b$ | 0.449 | 0.929 | 0.470 | 0.980 | 0.40 [29] | 0.560 [14] |
| | | | | | | 0.47 [38] | 1.711 [10] |
| $Zn_{1-x}Mg_xTe$ | $b_{VD}$ | −0.060 | −0.118 | | | | |
| | $b_{CE}$ | 0.809 | 1.403 | | | | |
| | $b_{SR}$ | 0.037 | 0.021 | | | | |
| | $b$ | 0.786 | 1.306 | 0.860 | 1.460 | 0.69 [39] | |
| | | | | | | 0.67 [9] | |

**Table 4.** Electron ($m_e^*$), light hole ($m_{lh}^*$) and heavy hole ($m_{hh}^*$) effective masses (in units of free electron mass $m_0$) at the Γ point of the Brillouin zone of the ternary alloys under investigation compared with the available experimental and theoretical predictions.

| | | $(m_e^*)_\Gamma$ | | | | $(m_{hh}^*)_\Gamma$ | | | $(m_{lh}^*)_\Gamma$ | |
|---|---|---|---|---|---|---|---|---|---|---|
| | | Present work | | | | Present work | | | Present work | |
| | $x$ | GGA | EVG | Exp. | Other work | GGA | EVG | Other work | GGA | EVG |
| $Zn_{1-x}Mg_xS$ | 1 | 0.267 | 0.323 | | 0.25 [13] | 2.643 | 2.904 | | 0.287 | 0.362 |
| | 0.75 | 0.261 | 0.340 | | | 1.774 | 1.978 | | 0.277 | 0.357 |
| | 0.50 | 0.247 | 0.321 | | | 1.523 | 1.717 | | 0.269 | 0.348 |
| | 0.25 | 0.215 | 0.278 | | | 1.197 | 1.31 | | 0.216 | 0.275 |
| | 0 | 0.185 | 0.245 | 0.341 [41] | 0.21 [13] | 1.174 | 1.283 | | 0.167 | 0.215 |
| $Zn_{1-x}Mg_xSe$ | 1 | 0.202 | 0.261 | | 0.24 [11] | 2.154 | 2.386 | 0.85 [11] | 0.215 | 0.287 |
| | | | | | 0.23 [13] | | | | | |
| | 0.75 | 0.191 | 0.260 | | | 1.478 | 1.629 | | 0.199 | 0.266 |
| | 0.50 | 0.173 | 0.236 | | 0.27 [11] | 0.999 | 1.110 | 1.47 [11] | 0.181 | 0.243 |
| | 0.25 | 0.144 | 0.198 | | | 1.042 | 1.135 | | 0.143 | 0.193 |
| | 0 | 0.114 | 0.163 | 0.147 [40] | 0.23 [11] | 1.020 | 1.108 | 1.44 [11] | 0.105 | 0.145 |
| | | | | | 0.17 [13] | | | | | |
| $Zn_{1-x}Mg_xTe$ | 1 | 0.181 | 0.236 | | | 1.571 | 1.728 | | 0.178 | 0.231 |
| | 0.75 | 0.188 | 0.261 | | | 1.115 | 1.231 | | 0.165 | 0.214 |
| | 0.50 | 0.164 | 0.229 | | | 0.960 | 1.066 | | 0.147 | 0.189 |
| | 0.25 | 0.129 | 0.176 | | | 0.812 | 0.887 | | 0.118 | 0.152 |
| | 0 | 0.099 | 0.139 | | | 0.797 | 0.869 | | 0.086 | 0.113 |

All terms presented in equation (8) were computed using GGA and EVGGA; for more computational details, we refer the reader to references [32, 33]. The calculated bowing parameters of the direct bandgap are presented in table 3. We note that the quadratic parameters

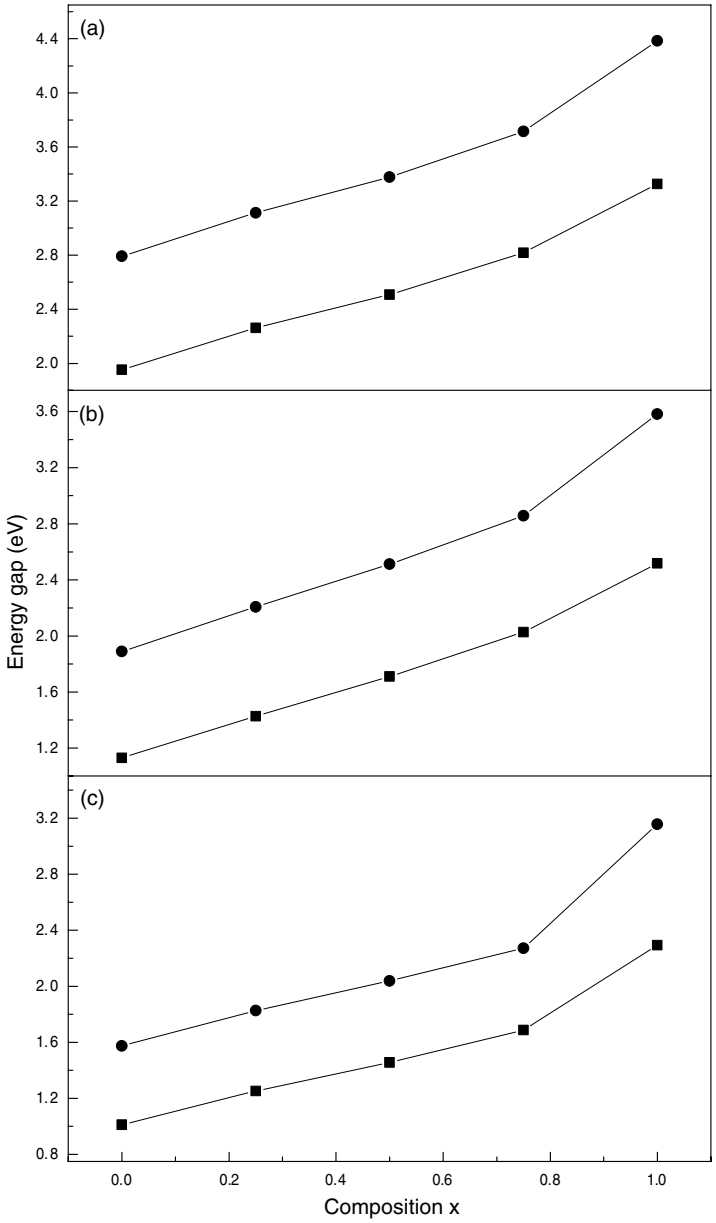


**Figure 4.** Direct bandgap energy $E_\Gamma^\Gamma$ as a function of Mg composition using GGA (solid squares) and EVGGA (solid circles) for (a) $Zn_{1-x}Mg_xS$, (b) $Zn_{1-x}Mg_xSe$ and (c) $Zn_{1-x}Mg_xTe$ alloys.

(gap bowing) calculated using GGA are in good agreement with experiment and very close to those of Zunger's approach. We conclude that the main contribution to the gap bowing is raised from the charge exchange effect. This can be clearly attributed to the large ionicity mismatch of the binary compounds.

It is also interesting to discuss at the end of the band structure study the effective masses of electrons and holes, which are important for the excitonic compounds. We have calculated the

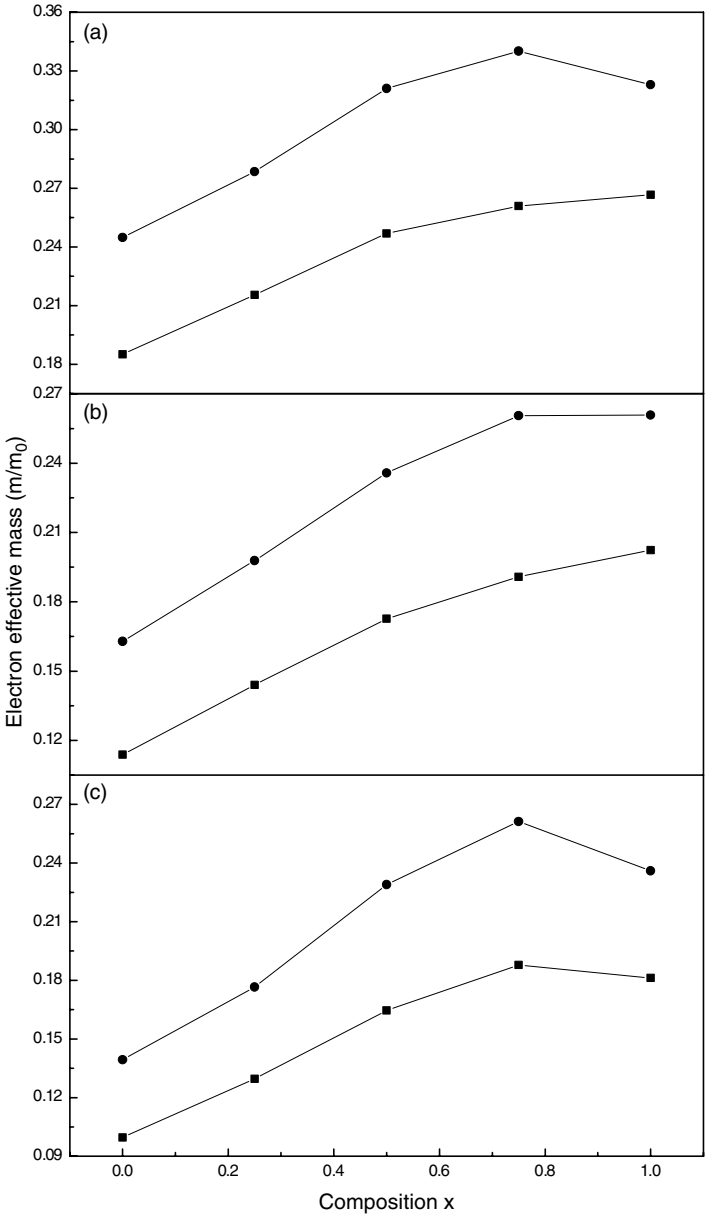


**Figure 5.** Electron effective mass (in units of free electron mass $m_0$) at the Γ point as a function of Mg composition using GGA (solid squares) and EVGGA (solid circles) for (a) $Zn_{1-x}Mg_xS$, (b) $Zn_{1-x}Mg_xSe$ and (c) $Zn_{1-x}Mg_xTe$ alloys.

effective masses of electrons and holes using both GGA and EVGGA schemes. A theoretical effective mass in general turns out to be a tensor with nine components. However, for a very idealized simple case where $E(k)$ is a parabola at $k = 0$ (high symmetry point Γ) the effective mass becomes a scalar. Our results concerning the electrons are displayed in figure 5. Accordingly, the electron effective masses at the Γ point increase non-linearly with increasing Mg concentration.

Table 4 lists our calculated electron and hole (heavy and light) effective masses at the Γ point of the Brillouin zone for $Zn_{1-x}Mg_xS$, $Zn_{1-x}Mg_xSe$ and $Zn_{1-x}Mg_xTe$ at various compositions. It is clearly seen that GGA values are smaller than the corresponding values within EVGGA. Our results calculated by the latter are in good agreement with the available experiment and also theoretical predictions.

## 4. Conclusions

Employing the FP-LAPW method, we have studied the composition dependence of the structural and electronic properties of $Zn_{1-x}Mg_xS$, $Zn_{1-x}Mg_xSe$ and $Zn_{1-x}Mg_xTe$ ternary alloys. We have optimized the lattice parameter for binary compounds as well as for alloys to find the ground state properties. For $Zn_{1-x}Mg_xS$ alloy the lattice constant closely follows Vegard's law, while for $Zn_{1-x}Mg_xSe$ and $Zn_{1-x}Mg_xTe$ a small deviation from Vegard's law with lattice bowing equal to $-0.03$ and $-0.02$ Å, respectively, has been observed. A significant deviation of the bulk modulus from LCD was found for all three alloys. This deviation is mainly due to the mismatch of the bulk modulus of binary compounds. The bulk modulus for the alloys of interest decreases on increasing the Mg concentration, which is due to the increase in the ionicity of bonds. Particular attention has been paid to the gap bowing, that exhibits non-linear behaviour versus the concentration. This latter is calculated using a simple interpolation scheme and also by following the approach of Zunger. The main contribution to the total bowing parameter rises from the charge transfer between anion and cation. In addition, we have computed the effective masses of the electron (hole), which increases with the composition $x$. Finally, our results could be useful for the design of blue and green–ultra-violet wavelength optoelectronic devices.

## Acknowledgment

Three of us (ZC, FEHH and HB) would like to thank the Physics Department of Isfahan University of Technology (IUT) as an ICTP Affiliated Center for their kind hospitality and financial support during the realization of this work.

## References

[1] Liu X and Furdyna J K 2004 *J. Appl. Phys.* **95** 7754
[2] Okuyama H, Nakano K, Miyajima T and Akimoto K 1991 *Japan. J. Appl. Phys.* **30** L1620
[3] Okuyama H, Kishita Y and Ishibashi A 1998 *Phys. Rev.* B **57** 2257
[4] Liu X, Bindley U, Sasaki Y and Furdyna J k 2002 *J. Appl. Phys.* **91** 2859
[5] Cavus A, Zeng L, Tamargo M C, Bamvpha N, Semendy A and Gray A 1996 *J. Appl. Phys.* **68** 3446
[6] Taniguchi S, Hino T, Itoh S, Nakano K, Nakayama N, Ishibashi A and Ikeda M 1996 *Electron. Lett.* **32** 552
[7] Firszt F 1993 *Semicond. Sci. Technol.* **8** 712
[8] Sallet V, Lusson A, Rommeluere M and Gorochov O 2000 *J. Cryst. Growth* **220** 209
[9] Watanabe K, Litz M Th, Korn M, Ossau W, Waag A, Landwehr G and Schüssler U 1997 *J. Appl. Phys.* **81** 451
[10] Benkabou F, Aourag H, Certier M and Kobayasi T 2001 *Superlatt. Microstruct.* **30** 9
[11] Charifi Z, Baaziz H and Bouarissa N 2004 *Mater. Chem. Phys.* **84** 273
[12] Charifi Z, Baaziz H and Bouarissa N 2004 *Int. J. Mod. Phys.* B **18** 137
[13] Teo K L, Feng Y P, Li M F, Chang T C and Xia J B 1994 *Semicond. Sci. Technol.* **9** 349
[14] Zaoui A 2002 *J. Phys.: Condens. Matter* **14** 4025
[15] Saitta A M, de Gironcoli S and Baroni S 1999 *Appl. Phys. Lett.* **75** 2746
[16] Saitta A M, de Gironcoli S and Baroni S 1998 *Phys. Rev. Lett.* **80** 4939
[17] Zunger A, Wei S-H, Feireira L G and Bernard J E 1990 *Phys. Rev. Lett.* **65** 353
Wei S-H, Feireira L G, Bernard J E and Zunger A 1990 *Phys. Rev.* B **42** 9622

[18] Blaha P, Schwarz K, Madsen G K H, Kvasnicka D and Luitz J 2001 *WIEN2K, An Augmented Plane Wave + Local Orbitals Program for Calculating Crystal Properties* Karlheinz Schwarz, Techn. Universitat, Wien, Austria (ISBN 3-9501031-1-1-2)
[19] Perdew J P, Burke S and Ernzerhof M 1996 *Phys. Rev. Lett.* **77** 3865
[20] Engel E and Vosko S H 1993 *Phys. Rev.* B **47** 13164
[21] Murnaghan F D 1944 *Proc. Natl Acad. Sci. USA* **30** 244
[22] Vegard L 1921 *Z. Phys.* **5** 17
[23] Vogle B, Morhain C, Urbaszeh B, Telfer S A, Prior K A and Cavenett B C 1999 *J. Cryst. Growth* **201** 950
[24] Madelung O (ed) 1982 *Londolt-Börnstein New Series Group III* vol 17 (Berlin: Springer)
[25] Lee S-G and Chang K J 1995 *Phys. Rev.* B **52** 1918
[26] Madelung O (ed) 1987 *Londolt-Börnstein New Series Group III* vol 22 (Berlin: Springer)
[27] Ley L, Pollak A, McFeely F R, Kowolczy S P and Shirley D A 1974 *Phys. Rev.* B **9** 600
[28] Franco R, Mori-Sánchez P, Recio J M and Pandey R 2003 *Phys. Rev.* B **68** 195208
[29] Jobst B, Hommel D, Lunz U, Gerhard T and Landwehr G 1996 *Appl. Phys. Lett.* **69** 97
[30] Dismuckes J P, Ekstrom L and Poff R J 1964 *J. Phys. Chem.* **68** 3021
[31] Charifi Z and Bouarissa N 1997 *Phys. Lett.* A **234** 493
[32] El Haj Hassan F and Akdarzadeh H 2005 *Mater. Sci. Eng.* B **121** 170
[33] El Haj Hassan F 2005 *Phys. Status Solidi* b **242** 909
[34] Zaoui A, Ferhat M, Khelifa B, Dufour J P and Aourag H 1994 *Phys. Status Solidi* b **185** 163
[35] Dufek P, Blaha P and Schwarz K 1994 *Phys. Rev.* B **50** 7279
[36] El Haj Hassan F, Akbarzadeh H and Hashemifar S J 2004 *J. Phys.: Condens. Matter* **16** 3329
El Haj Hassan F, Akdarzadeh H, Hashemifar S J and Mokhatari A 2004 *J. Phys. Chem. Solids* **65** 1871
[37] Szatkoski J, Firszt F, Meczunska H and Legowski S 1993 *Acta Phys. Pol.* A **84** 531
[38] Litz M Th *et al* 1996 *J. Cryst. Growth* **159** 54
[39] Seong M J, Alawadhi H, Miotkowski I, Ramdas A K and Miotkowska S 1999 *Solid State Commun.* **112** 329
[40] Holscher H W, Nothe A and Uihlein C 1985 *Phys. Rev.* B **31** 2379
[41] Kukimoto H, Shionoya S, Koda T and Hioki T 1968 *J. Phys. Chem. Solids* **29** 935
[42] Van Vechten J A and Bergstresser T K 1970 *Phys. Rev. Lett.* **31** 3351
[43] Wychoff R W G 1963 *Crystal Structures* 2nd edn, vol 1 (New York: Wiley) p 110
[44] Asano T A, Funato K, Nakamura F and Ishibashi A 1995 *J. Cryst. Gowth* **156** 373